iScience, Volume *26*

Supplemental information

Preclinical evaluation of a COVID-19 vaccine candidate based on a recombinant RBD fusion heterodimer of SARS-CoV-2

Antonio Barreiro, Antoni Prenafeta, Gregori Bech-Sabat, Mercè Roca, Eva Perozo Mur, Ricard March, Luis González-González, Laia Madrenas, Júlia Corominas, Alex Fernández, Alexandra Moros, Manuel Cañete, Mercè Molas, Thais Pentinat-Pelegrin, Clara Panosa, Alberto Moreno, Ester Puigvert Molas, Eva Pol Vilarrassa, Jordi Palmada, Carme Garriga, Teresa Prat Cabañas, Javier Iglesias-Fernández, Júlia Vergara-Alert, Cristina Lorca-Oró, Núria Roca, Leira Fernández-Bastit, Jordi Rodon, Mònica Pérez, Joaquim Segalés, Edwards Pradenas, Silvia Marfil, Benjamin Trinité, Raquel Ortiz, Bonaventura Clotet, Julià Blanco, Jorge Díaz Pedroza, Rosa Ampudia Carrasco, Yaiza Rosales Salgado, Jordina Loubat-Casanovas, Sara Capdevila Larripa, Julia Garcia Prado, Jordi Barretina, Marta Sisteré-Oró, Paula Cebollada Rica, Andreas Meyerhans, and Laura Ferrer

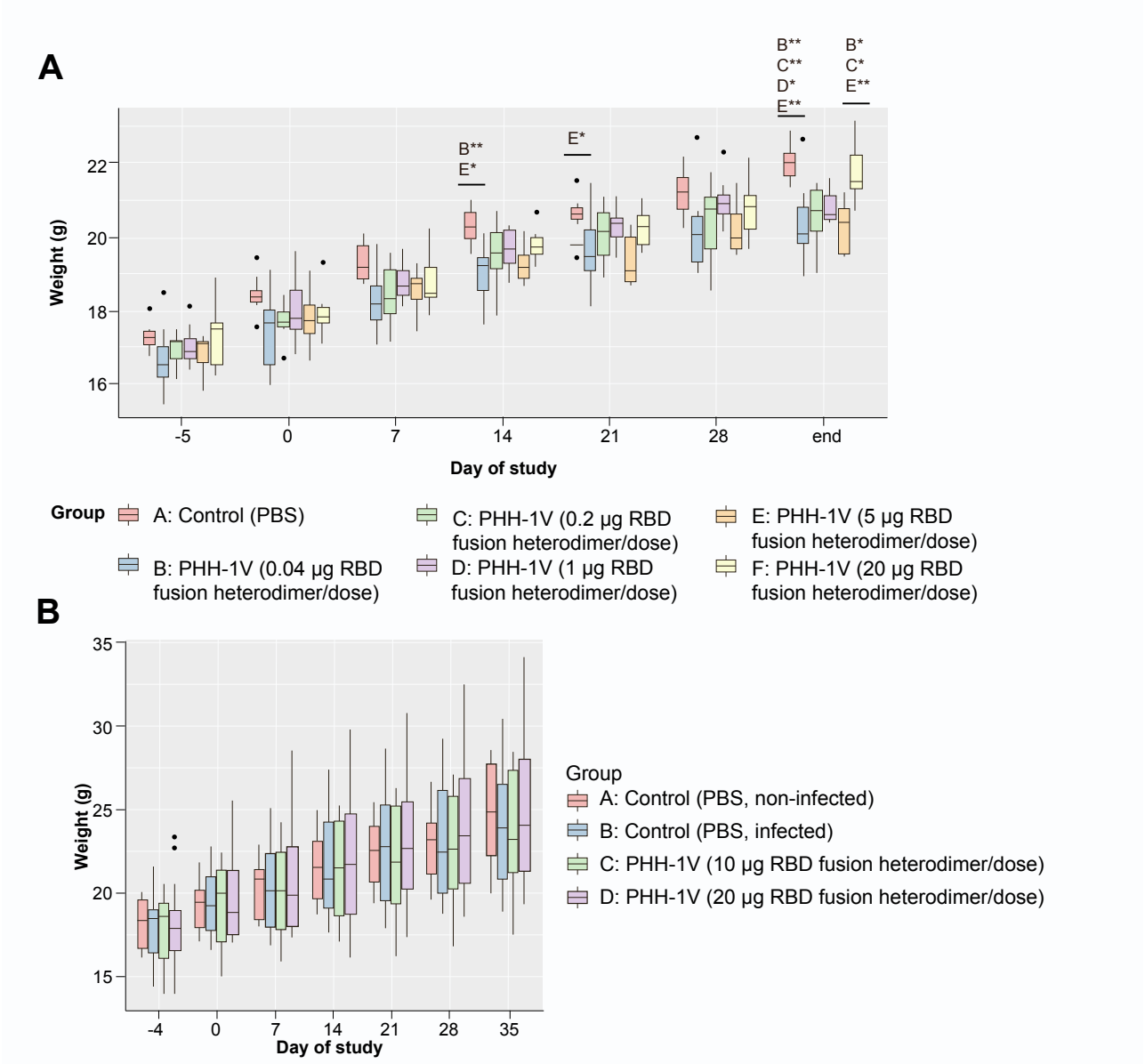

Figure S1. Bodyweight monitoring during the vaccination period in mice. Related to Figures 3-5. **(A)** Individual bodyweights in BALB/c mice. Mice were separated into different groups (8 mice/group): group A, vaccinated with phosphate-buffered saline (PBS) as a control group; group B, immunised with the 0.04-µg recombinant protein RBD fusion heterodimer/dose; group C, immunised with the 0.2-µg recombinant protein RBD fusion heterodimer/dose; group D, immunised with the 1-µg recombinant protein RBD fusion heterodimer/dose; group E, immunised with the 5-µg recombinant protein RBD fusion heterodimer/dose; and group F, immunised with the 20-µg recombinant protein RBD fusion heterodimer/dose. Data were analysed by ANOVA from D5 until the end of the study. Data are presented as a box plot: the median marks the midpoint of the data and is represented by the line that divides the box into two parts; the top and bottom limits of the box represent the first and third quartile, respectively; and the upper and lower whiskers represent the lowest and highest values of the distribution, except for the outliers (represented as dots). **(B)** Weekly individual bodyweights of each group during the vaccination period before SARS-CoV-2 infection in K18-hACE2 mice. Group A, vaccinated with PBS and non-infected (n=8, 4F + 4M); group B, vaccinated with PBS and infected with SARS-CoV-2 (n=18, 9F + 9M); group C, vaccinated with 10 µg/dose of recombinant protein RBD fusion heterodimer in oil-based adjuvant and infected with SARS-CoV-2 (n=18, 9F + 9M); and group D, vaccinated with 20 µg/dose of recombinant protein RBD fusion heterodimer in oil-based adjuvant and infected with SARS-CoV-2 (n=18, 9F + 9M). Data are presented as a box plot: the median marks the midpoint of the data and is represented by the line that divides the box into two parts; the top and bottom limits of the box represent the first and third quartile, respectively; and the upper and lower whiskers represent the lowest and highest values of the distribution, except for the outliers (represented as dots).

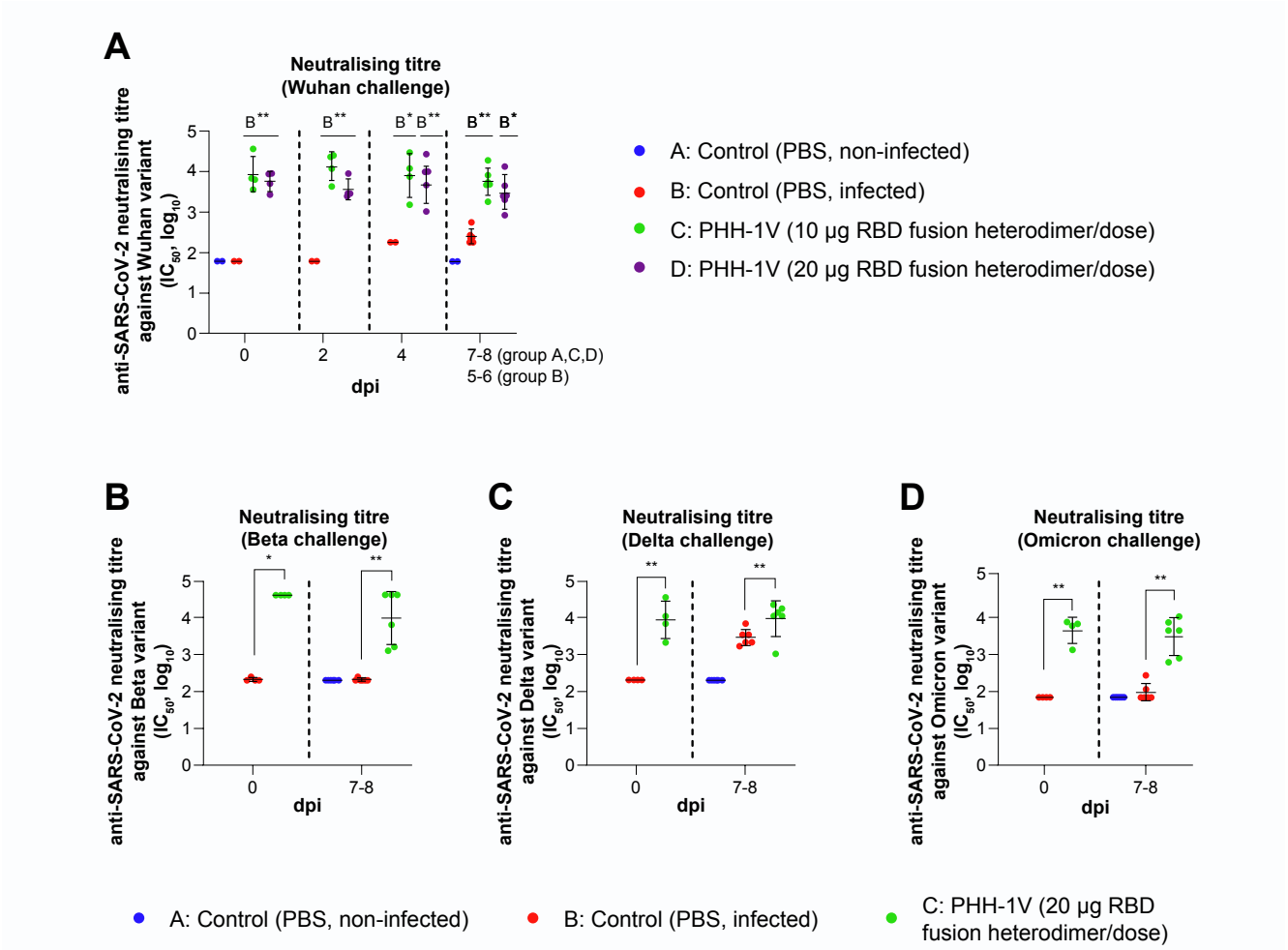

Figure S2. Neutralising antibody responses by PBNA in K18-hACE2 mice. Related to Figures 5-8. **(A)** Neutralising titres induced by PHH-1V against D614G Wuhan strain. Group A, PBS-vaccinated non-infected control (n=8); group B, PBS-vaccinated infected control (n=18); group C, vaccinated with 10 µg of recombinant protein RBD fusion heterodimer/dose and infected (n=18); and group D, vaccinated with 20 µg of recombinant protein RBD fusion heterodimer/dose and infected (n=18). Samples of groups A, C and D correspond to 0 (D35), 2 (D37), 4 (D39) and 7 dpi (D42 for males) or 8 dpi (D43 for females); samples of group B were taken 0 (D35), 2 (D37), 4 (D39), and 5 dpi (D40; n=3) or 6 dpi (D41; n=3), when animals reached the endpoint criteria. **(B-D)** Neutralising titres induced by PHH-1V against Beta **(B)**, Delta **(C)** and Omicron BA.1. **(D)** variants. Group A, PBS-vaccinated non-infected control (n=8); group B, PBS-vaccinated infected control (n=18); group C, vaccinated with 20 µg of recombinant protein RBD fusion heterodimer/dose and infected (n=18). All the samples correspond to 0 (D35), 2 (D37), 4 (D39) and 7 dpi (D42 for males) or 8 dpi (D43 for females or at the time of euthanasia in animals reaching endpoint criteria before the scheduled euthanasia day). Titres are expressed as log_{10} IC_{50}. Each data point represents an individual mouse serum, with bars representing the mean titre per group ± SD. These data were analysed using a generalised least squares model on the log_{10}-transformed values of each group. Statistically significant differences between groups are indicated with a line on top of each group: * *p<0.05;* ** *p<0.01*. dpi: days post-infection.

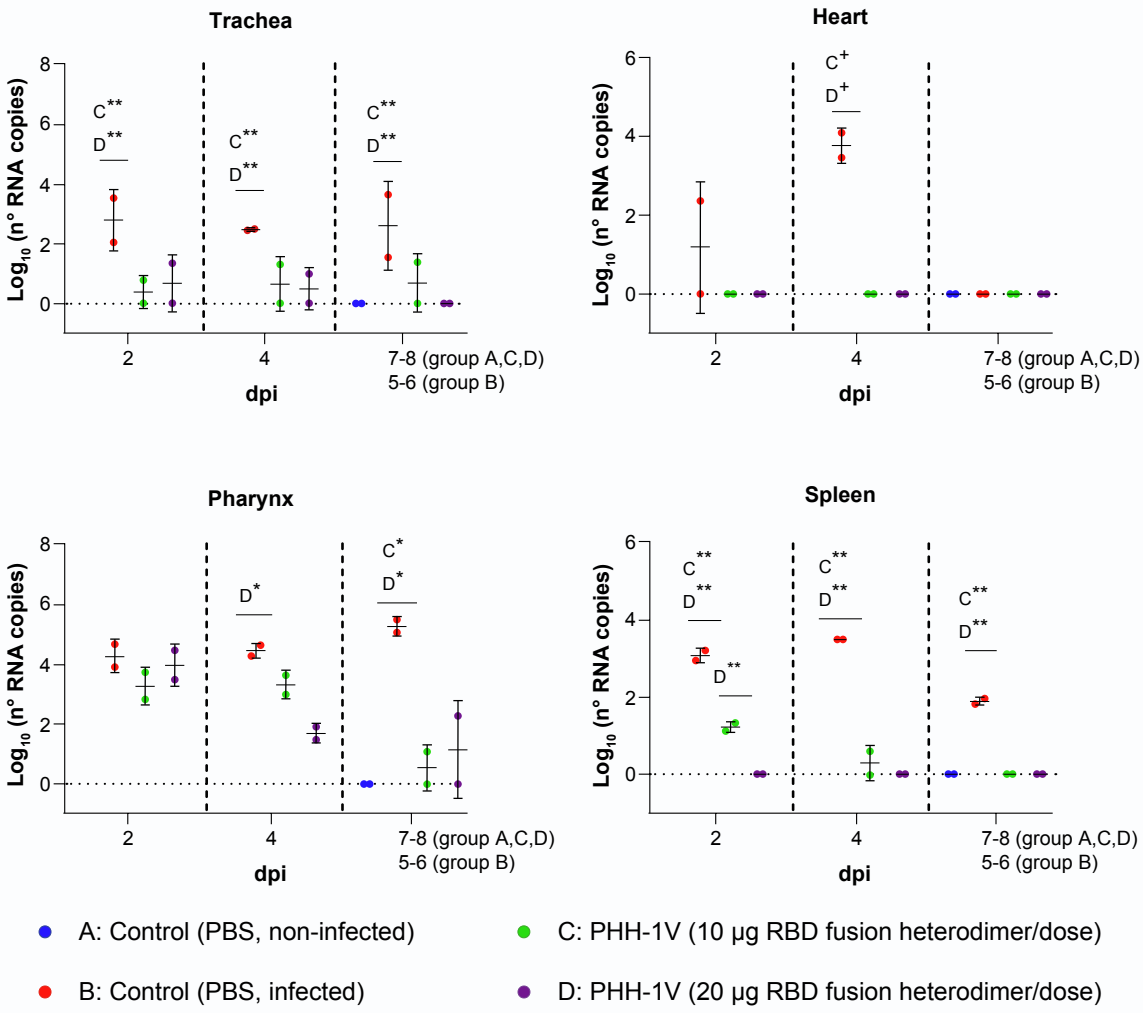

Figure S3. Viral load in different tissues from mice. Related to Figure 5. SARS-CoV-2 RT-qPCR detection in trachea, heart, pharynx and spleen in number of copies collected from challenged animals. Each data point represents an individual mouse value, with bars representing the mean ± SD. Samples of groups A, C and D correspond to 2 (D37), 4 (D39) and 7 dpi (D42 for males) or 8 dpi (D43 for females); samples of group B were taken 2 (D37), 4 (D39), and 5 dpi (D40; n=3) or 6 dpi (D41; n=3) when animals reached the endpoint criteria. These data were analysed using generalised least squares models on the log_{10}-transformed values of each group. Comparisons against groups without variability were performed by means of one-sample tests. Statistically significant differences between groups in the number of viral RNA copies are indicated with a line on top of each group: * $p<0.05$; ** $p<0.01$; $^{+}$ $0.05<p<0.1$. dpi: days post-infection.

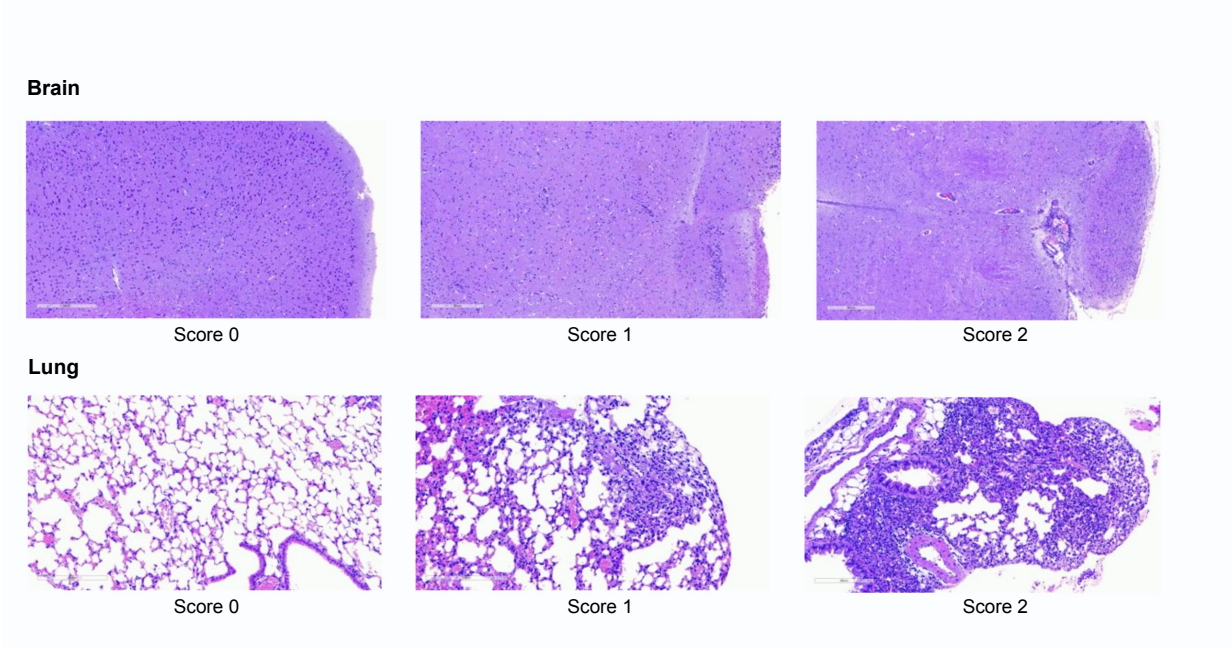

Figure S4. Representative brain and lung histopathological sections from K18-hACE2 transgenic mice euthanised at days 7-8 post-challenge. Related to Figure 5. Histopathological section stained with haematoxylin and eosin from brain (top) and lung (bottom) showing scores of 0 (lack of lesions), 1 (mild lesions), and 2 (moderate lesions). None of the study animals showed lesions with score 3 (severe lesions). The brain score section with a score of 0 comes from group A mouse at 7 dpi, the one with a score of 1 comes from group B mouse at 7 dpi, and the one with a score of 2 comes from a group B mouse at 4 dpi. The lung section with a score of 0 comes from group C mouse at 7 dpi, the one with a score of 1 comes from a group D mouse at 7 dpi, and the one with a score of 2 comes from a group B mouse at 4 dpi.

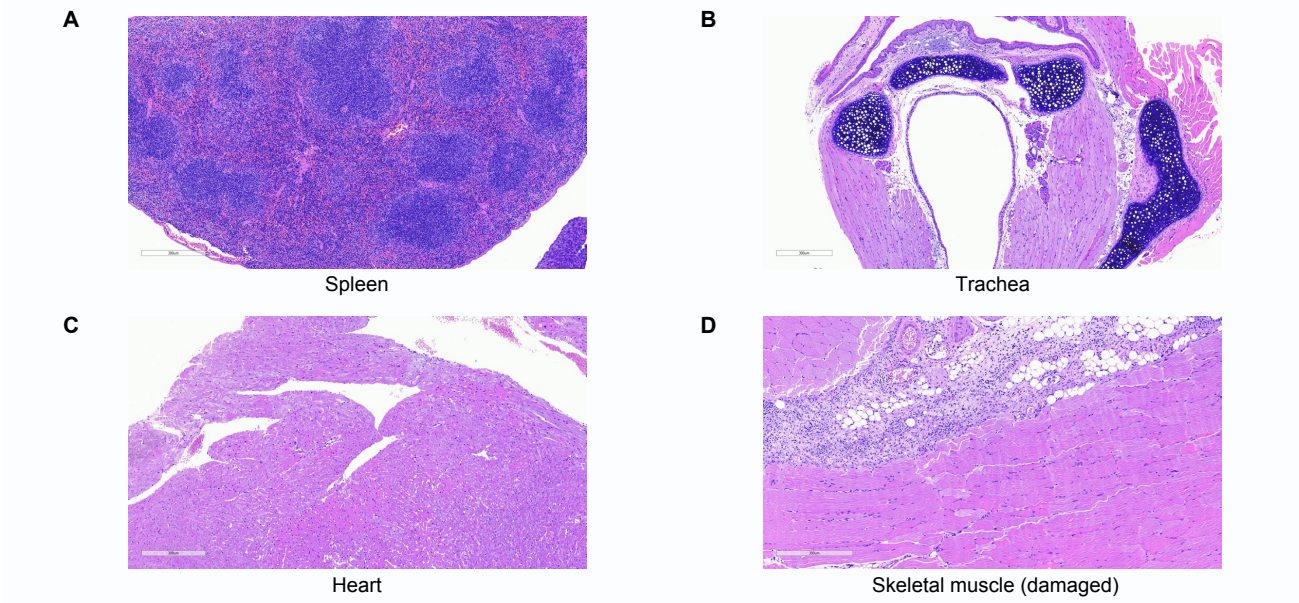

Figure S5. Representative histopathological sections from K18-hACE2 transgenic mice tissues. Related to Figure 5. No histopathological lesions were observed in spleen **(A)**, trachea **(B)** and heart **(C)** of SARS-CoV-2 Wuhan/D614G inoculated K18-hACE2 mice at days 7-8 post-challenge. **(D)** Focal mononuclear inflammatory infiltrates in the fascia around muscular fibres of a 20-µg RBD fusion heterodimer/dose on D4 post-challenge with SARS-CoV-2 Wuhan/D614G inoculated K18-hACE2 mice. Haematoxylin & Eosin stain. Bars = 300 micrometres.

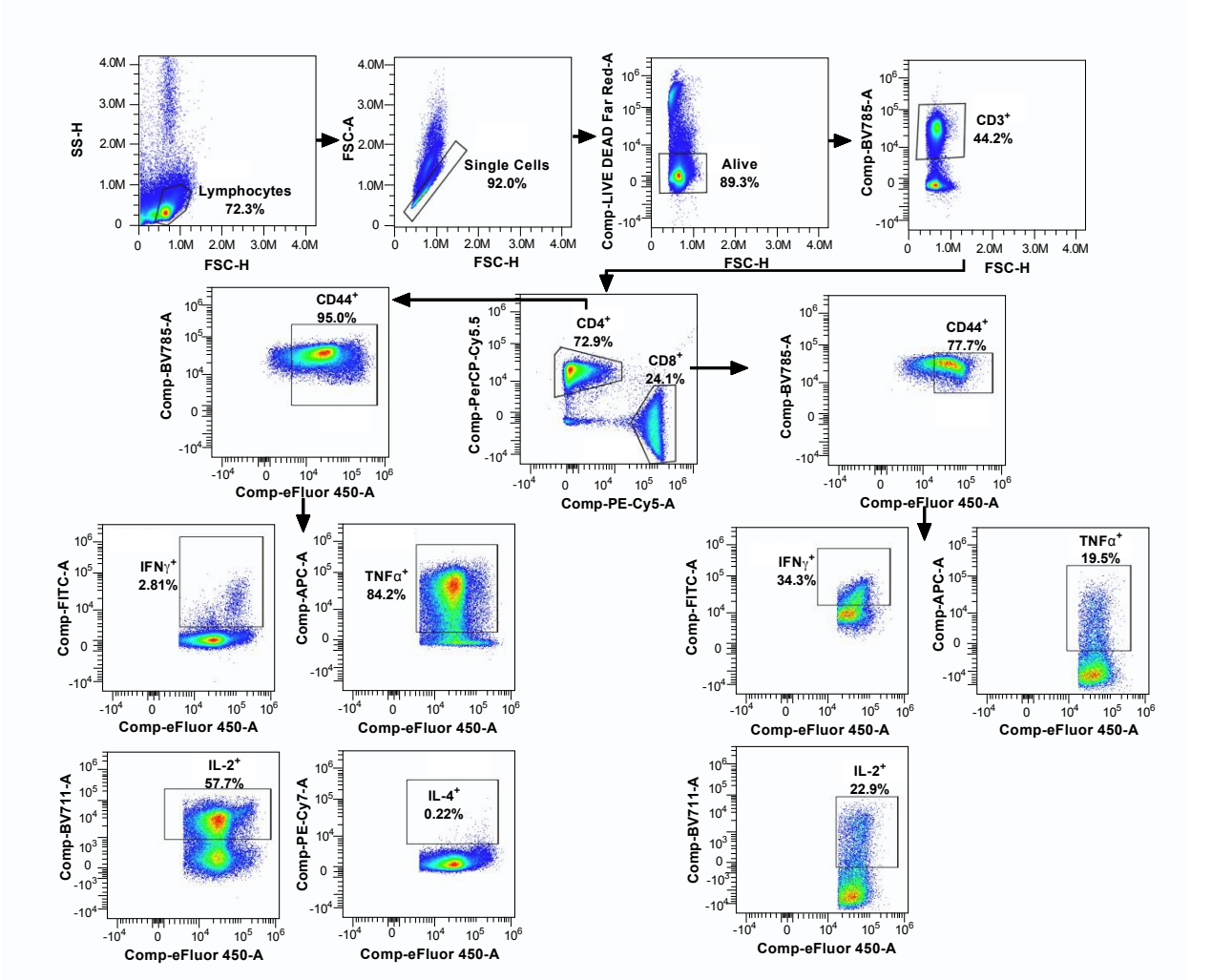

Figure S6. Identification of IFN-ɣ, TNF-α, IL-2 and IL-4-secreting CD4⁺ T cells and IFN-ɣ, TNF-α and IL-2-secreting CD8⁺ T cells from mice splenocytes using flow cytometry. Related to Figure 4. FSC-H/FSC-A was used to exclude doublets, and T cells (CD3⁺) within the alive cells (LIVE DEAD Far Red-) were gated. Then IFN-ɣ, TNF-α, IL-2 and IL-4-producing T cells upon mock or RBD-stimulation were measured from $CD4^+CD44^+$ and/or $CD8^+CD44^+$ populations. Fluorescence Minus One (FMO) controls were used to verify flow cytometry data.